Lab on a Chip

RSC Publishing

PAPER

View Article Online
View Journal | View Issue

Cite this: *Lab Chip*, 2013, **13**, 4078

In situ laser micropatterning of proteins for dynamically arranging living cells

Kazunori Okano,*[abcde] Ai Matsui,[b] Yasuyo Maezawa,[b] Ping-Yu Hee,[f] Mie Matsubara,[b] Hideaki Yamamoto,[g] Yoichiroh Hosokawa,[b] Hiroshi Tsubokawa,[d] Yaw-Kuen Li,[f] Fu-Jen Kao*[c] and Hiroshi Masuhara*[f]

Received 23rd June 2013,
Accepted 25th July 2013

DOI: 10.1039/c3lc50750e

www.rsc.org/loc

This study shows the modification of the surface of polymer-layered glass substrates to form biofunctional micropatterns through femtosecond laser ablation in an aqueous solution. Domains of micrometer size on a substrate can be selectively converted from proteinphobic (resistant to protein adsorption) to proteinphilic, allowing patterning of protein features under physiological aqueous conditions. When femtosecond laser pulses (800 nm, 1 kHz, 200–500 nJ per pulse) were focused on and scanned on the substrate, which was glass covered with the proteinphobic polymer 2-methacryloyloxyethylphosphorylcholine (MPC), the surface became proteinphilic. Surface analysis by X-ray photoelectron spectroscopy (XPS) and scanning electron microscopy (SEM) reveals that the laser ablates the MPC polymer. Extracellular matrix (ECM) proteins were bound to the laser-ablated surface by physisorption. Since femtosecond laser ablation is induced under physiological aqueous conditions, this approach can form micropatterns of functional ECM proteins with minimal damage. This method was applied to pattern collagen, laminin, and gelatin on the substrate. Removal of an ECM protein from the substrate followed by replacement with another ECM protein was achieved on demand at a specific location and time by the same laser ablation method. Living cells adhered to the fabricated domains where ECM proteins were arranged. The modification of patterning during cell culture was used to control cell migration and form arrays of different cells.

Introduction

Microarray devices such as DNA arrays,[1,2] protein arrays,[3–5] and cell arrays[6–8] play important roles in biological fields such as genomics and proteomics. Controlling the interaction and immobilization of functional biomaterials on the surface of a substrate is crucial to the development of biofunctional microdevices integrated with proteins, enzymes, and other components. Additionally, the use of living cells as functional elements is highly desirable for miniaturized laboratory-on-a-chip devices. When fabricating these microdevices, one important issue is the spatiotemporal control of protein adsorption and cell adhesion to the substrate.

Cell adhesion is mediated by extracellular matrix (ECM) proteins.[9–11] Hence, if the ECM proteins on a substrate are immobilized and patterned at a specific position and time during cell culturing, novel opportunities may be provided for studying many cellular processes such as cell division, differentiation, and migration. However, the patterns on a substrate surface must be dynamically modified to study such cellular processes.[9,11] Conversion of surface properties between cell adhesion and cell release can be achieved by using electrochemically reactive,[9,12,13] photochemically reactive,[14–17] enzymatically reactive,[18] and thermally responsive materials.[6,8] Moreover, photochromic substrates have been tested for their ability to switch between cell adhesion and cell release.[19,20] A bifunctional surface combining electroactive and photochemically active areas has been developed for stepwise immobilization of living cells and ligands at different locations to guide cell migration in ligand patterns.[21] Heterotypic cells have been arrayed by sequential activation of surface areas by ultraviolet (UV) light irradiation[14] or redox reactions.[13]

[a]*Center for Interdisciplinary Science, National Chiao Tung University, 1001 Ta-Hsueh Rd., Hsinchu 30010, Taiwan. E-mail: okano@nctu.edu.tw*
[b]*Graduate School of Materials Science, Nara Institute of Science and Technology, 8916-5 Takayama, Ikoma, Nara 630-0192, Japan*
[c]*Institute of Biophotonics, National Yang-Ming University, No.155, Sec. 2, Linong St., Beitou District, Taipei 112, Taiwan. E-mail: fjkao@ym.edu.tw*
[d]*Kansei Fukushi Research Institute, Tohoku Fukushi University, 6-149-1 Kunimigaoka, Aoba-ku, Sendai 989-3201, Japan*
[e]*Toin University of Yokohama, 1614 Kurogane-cho, Aoba-ku, Yokohama 225-8503, Japan*
[f]*Department of Applied Chemistry and Institute of Molecular Science, National Chiao Tung University, 1001 Ta-Hsueh Rd., Hsinchu 30010, Taiwan. E-mail: masuhara@masuhara.jp*
[g]*Waseda Institute for Advanced Study, Waseda University, 1-6-1 Nishiwaseda, Shinjuku-ku, Tokyo 169-8050, Japan*

Multiphoton laser ablation is effective for biomaterial patterning because of its minimal thermal effect on biological fabrications.[22,23] Healy's group showed that a covalently bonded polyethyleneglycol brush layer on a quartz substrate was ablated under atmospheric ambient conditions and patterned for neutravidin and integrin binding peptide to control the migration of living cells.[24] Similarly, a chemisorbed octadecylsiloxane self-assembled monolayer was ablated by a femtosecond laser, and structures $\leqslant$250 nm wide were fabricated.[25] Other direct patterning methods exist, such as laser-induced forward transfer (LIFT),[26] laser-assisted bioprinting (LAB),[27] or matrix assisted pulsed laser evaporation direct write (MAPLW DW).[28] The LIFT, LAB, and MAPLW DW methods use mechanical force generated by light absorption of a substrate, matrix, and the materials themselves to transfer biomolecules and living cells under ambient atmosphere. These methods use UV or infrared (IR) pulsed lasers. Our group developed a novel direct patterning method that applied a Ti:sapphire femtosecond laser with a matching biological window (700–900 nm) that limited damage to proteins and cells.[29,30] Functional proteins caged in insoluble particles[29] and cells[30] are released into the liquid by cavitation bubbles accompanied by mechanical force generated by the femtosecond laser. The proteins or cells were then transferred to the substrate, resulting in its patterning. To form tissue-like structures, three-dimensional arrangements of proteins and cells are important. One method for patterning ECM proteins was demonstrated by Gordon *et al.*[31] Three-dimensional engraving on a collagen gel by an intense femtosecond laser was used to fabricate a tissue scaffold. Holes, lines, and the grid in a collagen block were formed as scaffolds for cell culturing. Conversely, the femtosecond laser has been used to photocrosslink proteins for their patterning, where a photosensitizer (Rose Bengal, benzophenone dimer, or flavin adenine dinucleotide) was applied to make patterns of insoluble proteins.[32,33]

Although many studies of surface micropatterning for protein and cell arrays exist, the arrangement of multiple proteins and their replacement with other functional proteins under cell cultivation remains under development. Multiple patterning of functional proteins is necessary to induce active cellular networks. Additionally, patterning under physiological conditions is crucial to fabricate integrated protein devices. Although some methods achieved dynamic patterning, replacement of functional proteins or cells is still problematic. In actual organisms, cells divide, migrate, differentiate, and are replaced with other cells through their interactions. These cell functions are induced by many proteins, including ECM proteins. Collagen, laminin, fibronectin, myelin basic protein, and fibrin are related to both cell adhesion and differentiation. Some cells, such as neurons, require specific proteins to attach to solid surfaces.[10] Further, many proteins on a cell surface can induce cell–cell interactions and differentiation of other cells.[34] If one could array these functional proteins on a substrate at specific times, one could control the cell activity and cell–cell interactions on a device. Due to the complexity of protein-mediated cell adhesion and cell differentiation, controlling protein adsorption on a solid surface is essential to develop cell-based devices fabricated by patterning proteins and living cells. Functional proteins are easily denatured under dry conditions, and at the air–water interface. Previous studies did not always escape protein denaturation and cell damage. UV and IR irradiation, mechanical stress, chemical stress, heat, and desiccation affect proteins and living cells. For instance, fibronectin is sensitive to mechanical stress, which can cause it to form clots. As the photochemical, electrochemical, and enzymatic methods are carried out under aqueous conditions, these methods are attractive. They are also efficacious for one-time surface modification; however, more ideas are required for multiple modifications. In the case of laser direct patterning, the excimer laser is commonly used for patterning biological materials with a high resolution of sub micrometers, but this is only carried out in air or under vacuum pressure, which causes difficulty for *in situ* patterning under cell culturing. IR laser-based patterning carried out on a metal layer achieved *in situ* patterning in an aqueous condition. However, heat-sensitive proteins and cells are likely to be adversely affected by the laser. The effect of ablation on a metal layer and the produced nanometals remains unknown.

The novel approach in this work is based on surface modification through femtosecond laser ablation under aqueous conditions.[35] Multiphoton ablation of substrate materials using intense 800 nm pulses is applied to realize patterning under physiologically buffered conditions and under cell culturing. The 800 nm wavelength is located within the well-known biological window between the absorption bands of cellular materials and water. Moreover, the average energy is as low as 200–500 μW because of the short pulses. Therefore, multiphoton ablation using an intense 800 nm femtosecond laser is safe for ambient proteins and living cells, except for at the laser focal point. This is a superior characteristic to other laser-based patterning methods. This ablation method, which is applicable to many surface materials, enables spatiotemporal control of functional proteins on the surface under physiological conditions. In our previous report, femtosecond laser pulses were focused on a cytophobic surface coating to form channels several micrometers wide between cell adhesion domains.[35,36] The cells then elongated or migrated to connect with each other through these channels. During and after the laser patterning, the cells did not detach and die. This indicated that this method can form additional patterns during cell culturing because of the minimal damage to living cells. Thus, the pattern corresponding to cell behavior can be modifying, resulting in the control of cell division, migration, differentiation, and death. This is a new concept for future biological patterning.

This work developed a femtosecond laser-based *in situ* surface micropatterning method that forms small biofunctional domains covered with functional proteins, and is carried out fully in an aqueous solution. Patterns of laminin, collagen, and gelatin are formed on a substrate under aqueous

conditions. Sequential patterning of the ECM proteins collagen and laminin is demonstrated. Additionally, a patterned ECM is partially erased and replaced with a different ECM. The surface micropatterning mechanism is elucidated through analysis by X-ray photoelectron spectroscopy (XPS) and scanning electron microscopy (SEM), and experimentally using quantum dots (Q-dots) with negative and positive charge surfaces. Additional micropatterning during cell culturing is performed with normal human astrocytes (NHA) to control their migration. Plural cells (normal human keratinocytes (NHK) and cancerous HeLa cells) are arrayed by forming the cytophilic domains step by step. All processing is completed under physiologically buffered conditions; that is, during a culturing series in a medium. Further, *in situ* replacement of ECM proteins is demonstrated under aqueous conditions.

Results and discussion

Characterization of a micropatterned surface

First, the effects on the substrate when the femtosecond laser beam was focused on the substrate in water are elucidated. The substrate was glass layered with 2-methacryloyloxyethyl-phosphorylcholine (MPC) polymer[37] (MPC polymer-layered substrate). Fig. 1A and B are optical microscopic images and SEM images, respectively. The optical microscopic images were obtained when the laser scanned from right to left at 20 μm s^{-1} on the substrate. The left, middle, and right images are the beginning, intermediate, and end stages of laser scanning, respectively. Finally the 50 × 50 μm domain was irradiated by the laser beam. When the laser was focused on the water, continuous bubbles were generated. Therefore, the laser was focused to the plane where it did not generate bubbles by probing the focal point from the water phase to inside the substrate. This no-bubble-generation boundary plane was defined as the reference plane (Z = 0). Visible lines appeared on the substrate with 2 μm intervals because the laser was scanned with the same intervals. Visible lines were also observed when the laser was focused inside the substrate ($Z <$ 0; data not shown). Clearly, the femtosecond laser collapsed the glass. When the laser was focused on the water phase ($Z >$ 0), bubbles were generated vigorously by multiphoton absorption of the water. To elucidate the surface condition of the laser-treated domains, the surface was analyzed by SEM (Fig. 1B); the left and right substrates were prepared under different laser treatment conditions. When the femtosecond laser was focused at Z = −0.5 μm (left image), shadows (marked a in the SEM images) were observed along the laser scanned lines, which were clearly differentiated from their surroundings. We conclude that the surface of the MPC polymer-layered substrate was modified at the shadow areas. The width of each shadow line was 0.9 ± 0.1 μm (mean ± standard deviation), which was determined by measuring the cross-sectional profiles of the 19 lines. Since the laser lines ran at 2 μm intervals, an estimated 46% of the domain surface was modified. The right SEM image shows an entirely different aspect, where the laser was focused to a position shifted 0.5 μm relative to the water phase (Z = +0.5 μm). Many engraved

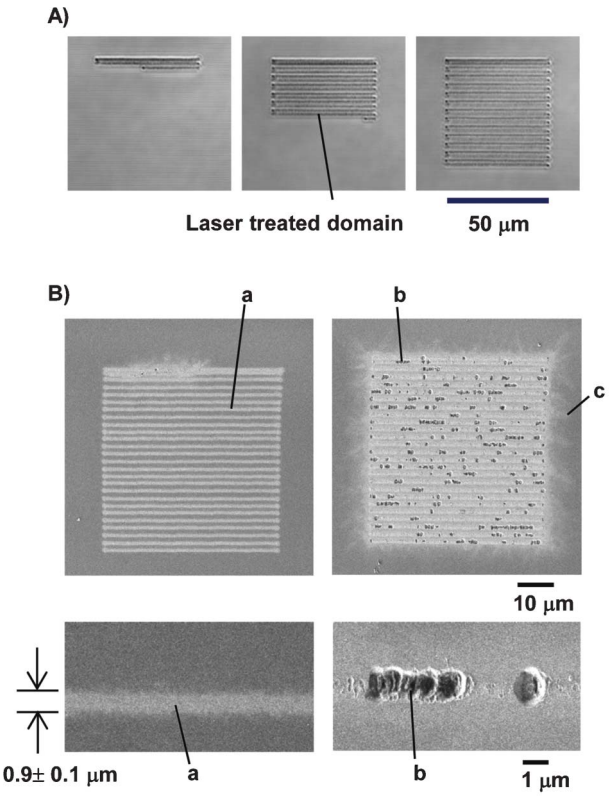

Fig. 1 The surface of the laser-irradiated MPC polymer-layered substrate. A) Optical microscope images of the MPC polymer-layered substrate during laser scanning at early, intermediate, and complete stages (left, middle, and right micrographs, respectively). The femtosecond laser (800 nm, 1 kHz, 0.2 mW) was focused with an objective lens (× 20, N.A. 0.46) on the MPC polymer-layered substrate immersed in water. B) SEM images of the laser-scanned surfaces of the MPC polymer-layered substrate. The femtosecond laser was focused at 0.5 μm inside the substrate (Z = −0.5 μm) (left), and at 0.5 μm in the liquid (Z = +0.5 μm) (right), where Z = 0 μm is defined as the position where bubble generation stopped when the focal point shifted from the water phase to the substrate solid phase.

areas existed on the laser-treated domain (marked as b), and were where the bubbles existed. Shadows were observed radially along the laser scanned lines (c), such that the boundary area of the modified domain and that around the MPC polymer-layered surface was unclear. This lack of definition and bubble generation will cause difficulty for the fine patterning of proteins or living cells. In conclusion, the MPC polymer-layered surface was likely modified at the laser-treated domain that is distinguished by a clear boundary area from its surroundings when the laser was focused inside the substrate near Z = 0. The substrate was roughened and damaged when the laser was focused near the substrate surface at $Z >$ 0.

Since the MPC polymer surface was changed by focused laser irradiation, second, the surface electrostatic potential of the laser-treated surface was evaluated. The main idea was to use fluorescent Q-dots with amino-, carboxy-, and non-dissociation groups, which have positive, negative, and neutral surface electric potentials under physiological pH, respectively. Fig. 2 shows an evaluation of the results. The laser was

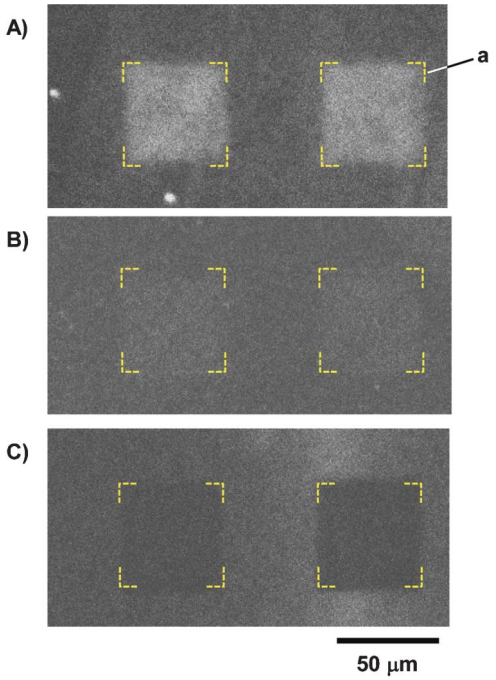

Fig. 2 Surface electrostatic properties of the laser-irradiated MPC polymer-layered substrate. Q-dots with A) amino, B) non-dissociation, and C) carboxy residues were incubated with the substrate for 16 h at 20 °C. The laser with a power of 0.5 mW was focused at the $Z = -0.5$ μm layer, where $Z = 0$ μm is defined as the position where bubble generation stopped after shifting the focal point from the water phase to the substrate solid phase. The domains (a) surrounded by yellow brackets were irradiated by the femtosecond laser.

focused to the plane $Z = -0.5$ μm and used to irradiate 50 × 50 μm domains on the MPC polymer-layered substrates in water. Each substrate was covered with each Q-dot solution, and then incubated for 16 h at 20 °C. The fluorescence images were acquired after the substrate was replaced with fresh buffer solution without Q-dots. The intact MPC polymer-layered surface did not adsorb the Q-dots (outer area of dotted yellow line a). The laser-irradiated domains adsorbed the Q-dots with amino residues well (A), while the same surface only slightly adsorbed the Q-dots with non-dissociation residues (B), and minimally adsorbed the Q-dots with the carboxy group (C). The modified surface was now interacting with Q-dots with amino residues. The distinguishing characteristic of these three Q-dots is their electrostatic surface charges. The experiment was conducted under the physiological pH of 7.4. Because Q-dots with amino residues are protonated and positively charged under this condition, the laser-treated surface has negative potential. Conversely, the zwitterionic MPC polymer-layered surface prevents adsorption of any Q-dots because such a surface interacts minimally with particles that have both negative and positive charges.[37]

Third, in this work we analyzed the chemical elements by XPS (Table 1) to define the surface negative potential of the laser-treated domain. The 1.5 × 1.5 mm domain on the MPC polymer-layered surface was treated with a focused femtosecond laser under the condition of $Z = 0$ in water for XPS analysis. Notably, Si was not detected on the MPC polymer-layered surface, while Si accounted for 31.4% of the glass surface (molecular ratio). The Si was recovered to 15.7% on the laser-treated domain. Carbon content decreased from 62.4 to 34.8% following femtosecond laser irradiation. The experimental data show that 44–50% of the MPC polymer-layered surface disappeared, which agrees with the SEM result (46% of the MPC polymer-layered surface was modified). Additionally, new components that belong to oxidized carbon were detected at 291.0 and 293.4 eV. This oxidized carbon amounts to 2.2% of the remaining carbon on the substrate surface. It has been reported that carboxy or other oxidized residues are produced when an excimer laser (248 nm) irradiates polymethylmethacrylate polymer in air.[38] The femtosecond laser used here was powered at 0.2–0.5 mW (at 1 kHz), which amounted to 200–500 nJ per pulse to induce multiphoton adsorption of 266–160 nm (3–5 photons). The MPC polymer on the substrate may be oxidized photochemically. All the data indicate that the MPC polymer was ablated by the femtosecond laser under aqueous conditions. Consequently, the femtosecond laser exposed the bare glass surface. The glass surface immersed in neutral pH solution has negative surface charges, primarily generated through the dissociation of terminal silanol groups.[39,40] Hence, the fact that the positively charged Q-dots with amino residues strongly interacted with the laser-treated surface (Fig. 2) can be explained by the fact that the MPC polymer-coated surface was ablated by the femtosecond laser.

Table 1 XPS surface analysis

Elements	Binding energy/eV	Surface amount/mol%		
		Laser (−)[a]	Laser (+)[a]	Glass
C 1s	284.8	34.8	17.3	6.0
	286.2	20.5	12.2	0
	288.6	7.1	4.5	0.9
	291.0	0	0.4	0
	293.4	0	0.4	0
N 1s	402.2	2.7	2.0	0.1
O 1s	529.8	3.3	0	0
	532.1	26.4	45.3	61.6
P 2p	133.4	5.2	2.2	0
Si 2p	102.8	0	15.7	31.4

[a] Laser (−) and (+) means the MPC polymer surface before and after laser-treatment, respectively.

The laser focal position was predicted as critical for the surface ablation because the ablation is due to multiphoton absorption, where different events were observed near the water–substrate surface. Hence, the best focal position was determined using fluorescent collagen (Alexa Fluor 488 collagen). The laser exposed the glass surface, such that fluorescent collagen was easily adsorbed. The fluorescence intensity from fluorescent collagen adsorbed on the laser-treated domains was determined under various focus conditions in the range of -4 μm $\leqslant Z \leqslant 2$ μm. If the laser ablated the MPC polymer efficiently, strong fluorescence would be clearly observed. Poor efficiency would give weak fluorescence. Fig. 3 shows the results. Fluorescence was observed from the domains irradiated by the focused femtosecond laser at ranges of $Z > -3$ μm and $Z > -2$ μm with laser powers of 0.5 mW and

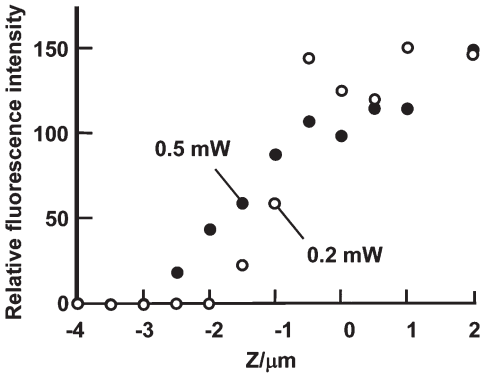

Fig. 3 Effect of laser focal point on ablation of the MPC polymer layer on the substrate. Alexa Fluor 488 collagen was used to treat the laser-irradiated MPC polymer-layered substrates. The fluorescence intensity obtained from the laser-irradiated area is plotted against laser focal point (*Z*), where minus and plus values may correspond to irradiation inside the glass and in solution, respectively. Notably, $Z = 0$ μm is defined as the position where bubble generation stopped after shifting the focal point from plus to minus. Fluorescence is due to Alexa Fluor 488, which was introduced to the surface. Open and closed circles represent laser powers of 0.2 and 0.5 mW, respectively.

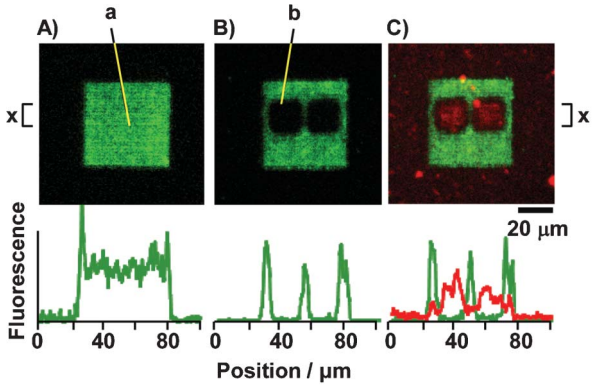

Fig. 4 Demonstration of multiple ECM patterning. Domains colored green and red were ablated and then covered with Alexa Fluor 488 collagen and Alexa Fluor 555 laminin, respectively. Fluorescence profiles are acquired by probing its intensity from left to right for the width of *x*. A) The femtosecond laser was first drawn at the domain a (50 × 50 μm), and then the substrate was treated with collagen (0.2 μM, PBS, pH 7.4, 16 h). B) The laser was focused onto the collagen-adsorbed domain b (15 × 15 μm) of the substrate prepared above. C) The substrate was treated with laminin (0.2 μM, PBS, pH 7.4, 16 h). The femtosecond laser (0.5 mW) scanned the substrate with a 1 μm interval.

0.2 mW, respectively, resulting in ablation of the MPC polymer in these ranges. Fluorescence intensity was as low as the background level when the laser was focused to the lower plane of those *Z* values. Relatively stronger fluorescence was observed when the laser was focused nearer $Z = 0$ μm, which is defined as the reference focal plane. At a range of $Z > 0$ μm, the substrate surface was devastatingly damaged, as in some SEM images. Thus, the range of the focal position was critically narrow for micropatterning of the MPC polymer-layered surface. The recommended range of the focal position for laser ablation is as narrow as $-0.5\ \mu m \geqslant Z \geqslant 0\ \mu m$.

Micropatterning ECM proteins by femtosecond laser ablation

The MPC polymer layer on the substrate was ablated by the femtosecond laser in an aqueous solution, on which positively charged particles and collagen were adsorbed. To assess the performance of micropatterning of functional proteins by this femtosecond laser ablation method under physiological buffered conditions, multiple proteins were patterned on a substrate. Two fluorescent proteins (Alexa Fluor 488 collagen and Alexa Fluor 555 laminin) were prepared for multiple protein patterning. This multiple patterning method has three steps: A) formation of an Alexa Fluor 488 collagen pattern on the substrate; B) partial ablation of the attached Alexa Fluor 488 collagen from the substrate; and C) formation of an Alexa Fluor 555 laminin pattern at the collagen-ablated domains on that substrate (Fig. 4). The MPC polymer-layered substrate surface was irradiated with the focused femtosecond laser in phosphate-buffered saline (PBS) containing Alexa Fluor 488 collagen. The laser was focused to the surface ($Z = 0$ μm) of the MPC polymer-layered substrate through the glass phase with an inverted microscope. After laser irradiation, the substrate was left in the same solution for 16 h, and washed with PBS before fluorescence imaging. Fluorescence from the laser-irradiated domain was clearly distinguishable from the remaining surrounding MPC polymer areas (A). Thus, the Alexa Fluor 488 collagen was preferentially adsorbed on the laser-irradiated domain. The femtosecond laser was again used to treat the collagen-adsorbed domain in PBS. The fluorescence of the laser-treated domains disappeared (B). The Alexa Fluor 488 collagen was ablated and removed from the laser-irradiated domain. Next, the substrate was incubated in PBS containing Alexa Fluor 555 laminin for 16 h and the solution was then replaced with pure PBS. Fluorescence from the Alexa Fluor 555 was emitted from the laser-ablated domain. The Alexa Fluor 555 laminin was adsorbed by the laser-treated domains. The domains of Alexa Fluor 555 laminin were clearly distinguishable from those of Alexa Fluor 488 collagen by fluorescence spectroscopic observations (C). These fluorescence results indicate that the proposed femtosecond laser-ablation technique can prepare various domains covered with various proteins under physiological buffered conditions. Furthermore, a domain once covered with protein can be erased and converted spatiotemporally into a surface with a different protein.

Living cell arrangement by femtosecond laser ablation

The femtosecond laser thus modifies the micropattern of ECM proteins under aqueous conditions, implying that the micropattern can be modified during live cell cultivation. Our interest is control of cell–cell interactions. This work will show that using laser ablation to modify a pattern is efficacious in controlling cell migration and the arrangement of different cells.

The collagen pattern was modified into an array of NHA to observe the migration behavior of the NHA (Fig. 5). Domains of a wide rectangle (100 × 2000 μm) and 12 squares (70 × 70 μm) were formed by a femtosecond laser in collagen solution (0.1 μM), such that the domains were covered with collagen (A). The NHA adhered well through the collagen layer onto the domain surface. The same cells adhered only minimally when

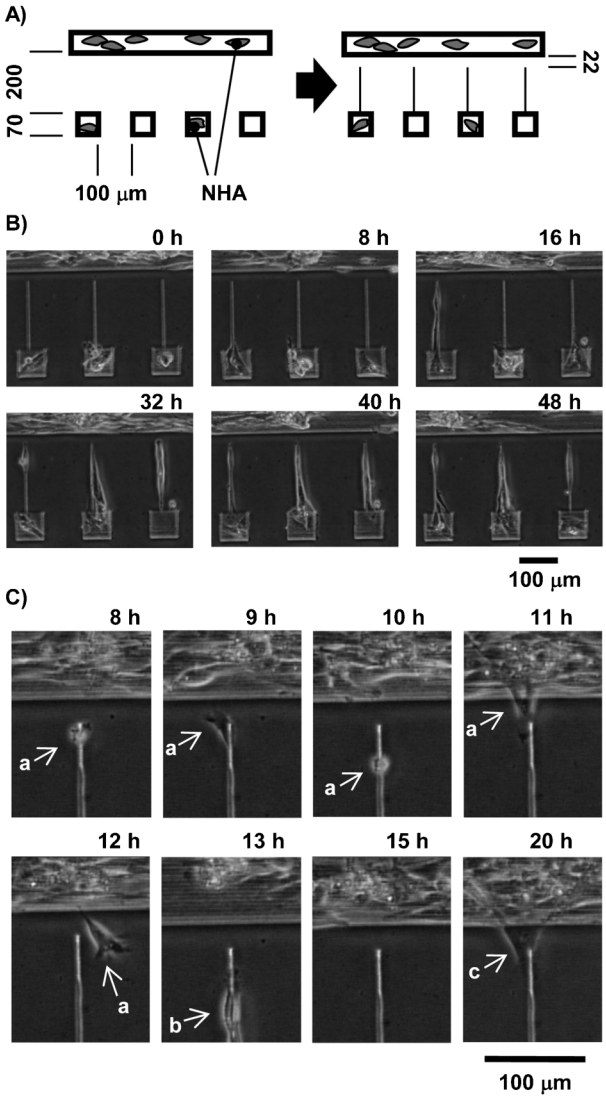

Fig. 5 Behavior of NHA on the patterned substrate. A) Schematic illustrations of patterns. First, the MPC polymer-layered substrate was patterned with femtosecond laser ablation, and then NHA were seeded (left). The substrate was then patterned again under the cell culture conditions as illustrated (right). Laser ablation was carried out in collagen solution. The series of photographs B) and C) are time-lapse images of NHA on the micropatterned substrate, in which the NHA remained in the channels and cells passed through gaps, respectively.

surface patterning was done in medium without collagen. Thus, collagen is necessary to array NHA on the femtosecond laser-patterned substrate. Cells adhered to the large rectangular domain and on 8 of the 12 small square domains. The other 4 square domains were empty. After the NHA adhered to the domains, the substrate surface was again modified by the femtosecond laser in the same collagen solution. All the square domains now bordered the rectangular domain with narrow channels (3 μm wide) with gaps of 22 μm. During this additional modification, the cells remained in their original positions. The cells were monitored by time-lapse imaging (B). The NHA that adhered to the 8 square domains moved into the channels. The additional modification after cell seeding is necessary to control migration because cells adhere directly to the lines when all patterns are prepared before cell seeding. The NHA migrated to and invaded the narrow channels from the wide 70 × 70 μm domains with high probability in the experiment. A similar experimental result was obtained for HeLa cells. In real organisms, cells migrate to change their position to express their functions during histogenesis. For instance, young neurons change position by migrating through astrocytic tunnels.[41] Similar to this phenomenon *in vivo*, control of cell migration on a patterned substrate may be useful for the study of cell reforming in tissues. The physical space seems important to cellular migration. The NHA stayed in 6 of the channels. However at two positions, the NHA extended filopodia to the cytophobic surface made by the MPC polymer and passed through the gaps by frequently elongating and reducing their soma (cell indicated with a in micrograph C). Attack of the next cell b was incomplete, while the latter cell c passed through the gap. No cells migrated between the square domains separated by 100 μm gaps. The front of the NHA body can likely probe an area of about 25 μm.

Finally, the arrangement of different cells by applying the proposed *in situ* surface patterning technique is demonstrated. HeLa cells and NHK were arrayed on a MPC polymer-layered substrate (Fig. 6). Cell adhesion domains (50 × 50 μm) were formed step by step, as shown in schematic illustration A. The substrate was placed in a medium containing gelatin (1 mg ml^{-1}) as an ECM-like protein for the entire patterning process. Thus, we assume the laser-ablated domains are covered with a gelatin layer, similar to laser-ablated domains with collagen adsorption (Fig. 4). To reduce the patterning time, the cells were immediately seeded after the laser-ablation process. Photograph B shows a resulting arrangement of NHK and HeLa cells. When NHK were seeded on the substrate and incubated overnight, the cells adhered to the laser-drawn domain, but not to the MPC polymer area (B-1). After removing un-adhered cells, another laser-ablated domain was formed adjacent to the former domain (B-2). A HeLa cell, which was cultured in advance on a different culture plate, was detached and translocated to the newly formed cytophilic domain. The HeLa cell adhered on the new domain (B-3) and migrated to the domain of the NHK , finally adhering to the domain of the NHK (B-4), and lasting there for several days. Since the medium differed for NHK and HeLa cells, both cells were too delicate to adhere on the laser-ablated area without gelatin under co-culturing, inducing cell death. Coating with the ECM protein (the gelatin) was hence indispensable to enhancing the adhesion of different cells to laser-ablated domains. HeLa cells adhered and spread their filopodia on the glass well in Dulbecco's Modified Eagle Medium (DMEM) containing fetal bovine serum (FBS), regardless of whether the ECM was included. Conversely, HeLa cells spread filopodia weakly in the culture medium for NHK without an ECM. The HeLa cells migrated little under the medium condition for NHK. Meanwhile, the morphology of the NHK changed to round in DMEM containing FBS. Although the two media were mixed, the adhesion activity of the cells remained weak without the ECM. Co-culturing NHK and HeLa cells on the patterned substrate succeeded in medium containing gelatin as an ECM-like protein. Thus, the ECM on the patterned domain is necessary for patterning different cell types on a substrate.

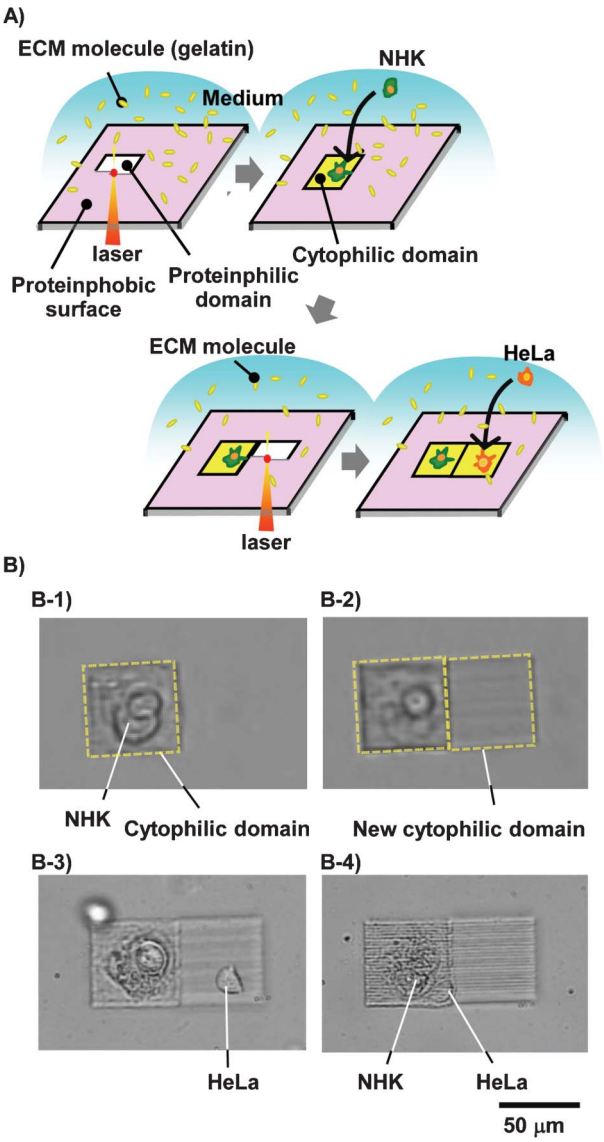

Fig. 6 Co-culture of a HeLa cell close to NHK on a patterned substrate. A) Schematic illustrations of *in situ* micropatterning for a co-culture of NHK and a HeLa cell. A small domain of the MPC polymer-layered surface is ablated by a femtosecond laser in a culture medium containing ECM protein (gelatin). The ECM molecules are adsorbed on the laser-ablated proteinphilic domain. The NHK then adhere to the ECM-adsorbed cytophilic domain. A new cytophilic domain is formed next to the NHK, and a HeLa cell is arranged. B) Microscopic images of the HeLa cell and NHK on the substrate. B-1) A square cytophilic domain was prepared on the MPC polymer-layered substrate by femtosecond laser ablation. The NHK adhered to the cytophobic domain. B-2) A new cytophilic domain was formed neighboring the NHK-adhered domain by the same laser ablation. B-3) A HeLa cell was spread on the newly formed domain. B-4) The HeLa cell and NHK were co-cultured for 2 days. The cytophilic domains (50 × 50 μm) were formed by applying the femtosecond laser (0.5 mW) with a 2 μm interval.

Conclusions

This work elucidated the mechanism of femtosecond laser-based surface modification under aqueous conditions. The physisorbed MPC polymer on glass was oxidized and ablated by the femtosecond laser. The ECM proteins (collagen, laminin, and gelatin) were then adsorbed onto the ablated domains. The receptors on cells identify the ECM molecules to complete cell adhesion. The proposed surface modification technique is applicable to many surfaces. The proteinphobic (cytophobic) surface of the MPC polymer was successfully converted to a proteinphilic (cytophilic) surface under physiological aqueous conditions by femtosecond laser ablation. The most significant benefit of this method is that the protein layered on a surface can be replaced by another protein repeatedly under physiological aqueous conditions because the proposed method is based on *in situ* laser ablation. This approach is superior to chemical modification methods that utilize conventional enzymatic, redox, or photocleaving reactions. By applying surface ablation patterning, various cells were arrayed successfully. Since it is possible to form a layered substrate that has different ECM proteins, one can array and co-culture cells requiring different ECMs. The *in situ* laser micropatterning of proteins will uniquely contribute to the study of many cellular processes related to cell division, differentiation, and migration. For instance, integrated cell devices made of neurons, astrocytes, and vascular cells, which are formed by this *in situ* micropatterning method, will prove useful when studying the plasticity of the neuronal circuit, because the proposed method can switch their circuit dynamically.

Experimental section

Materials

MPC polymer (Lipidure-CM5206) was kindly provided by NOF Corporation (Tokyo, Japan). The following proteins and chemicals were used without further purification: Cellmatrix type 1C collagen, gelatin (APH-100) (Nitta Gelatin Osaka, Japan), laminin-1, Alexa Fluor 488 succinimidyl ester and Alexa Fluor 555 succinimidyl ester, Qdot® 585 ITK™ Carboxyl Quantum Dots, Qdot® 585 ITK™ Amino (PEG) Quantum Dots, and Qtracker™ 565 non-targeted Quantum Dots (Invitrogen/Life Technologies). Cells and culture medium were as follows: HeLa cells (RCB0007, Riken Cell Bank, Tsukuba, Japan), NHK (KK-4009) and its medium kit with growth supplements (EpLife-KG2) (Kurabo, Osaka, Japan); NHA (CC-2565) and its medium kit with growth supplements (CC-3186) (Lonza, Walkersville, MD, USA); Dulbecco's Modified Eagle Medium (DMEM), fetal bovine serum (FBS), horse serum (HS), and mixed antibiotic solutions of streptomycin and penicillin (GIBCO/Life Technologies). Commercially provided materials were as follows: cell culture plastic wares (Asahi Glass, Funabashi, Japan); glass substrate (8 × 8 × 0.4 mm, Matsunami Glass, Kishiwada, Japan); ultrafiltration device (Cut off Mr mass; 30 kDa, OD030C33, Pall).

Preparation of fluorescent ECM proteins

Alexa Fluor 488 collagen was prepared as follows. Alexa Fluor 488 succinimidyl ester (5 μl, 10 mM, dissolved in DMSO) was mixed with a collagen solution (100 μl, 10 μM dissolved in 1

mM HCl). The reaction was initiated by adding 100 μl 0.1 M sodium phosphate buffer (pH 8.0). After incubation for 2 h, the Alexa Fluor 488 collagen was recovered by an ultrafiltration device. The purified Alexa Fluor 488 collagen (4 μM in 1 mM HCl) was stored at 4 °C.

Alexa Fluor 555 laminin was prepared as follows. Laminin-1 (400 μg, 400 μl) dissolved in 0.1 M sodium phosphate buffer (pH 8.0) was mixed with 5 μl Alexa Fluor 555 succinimidyl ester (10 mM, dissolved in DMSO) for 30 min. The Alexa Fluor 555 laminin was purified by ultrafiltration and stored in PBS (pH 7.4) at 4 °C (concentration of 0.6 μM).

Preparation of the MPC polymer-layered substrate

The MPC polymer was dissolved in ethanol to 0.1% and filtrated through a 0.2 μm membrane. Borosilicate glass plates (10 × 10 × 0.4 (t) mm) were cleaned with a hot solution of H_2O_2 (10%) and NH_4OH (10%) at 70 °C for 30 min and rinsed with distilled water. The glass plates were immersed in an ethanol solution of the MPC polymer (0.1%) for 1 min and then dried in air. The MPC polymer-layered substrate can be stored in clean air for over 1 month. The prepared MPC polymer-layered substrate was immersed in water overnight before use.

Surface patterning of the MPC polymer-layered substrate by femtosecond laser ablation

Surface modification and patterning was achieved by femtosecond laser ablation, as previously reported.[35] The femtosecond laser (800 nm, 1 kHz, 0.2–0.5 mW) from a regenerative amplified Ti:sapphire laser (Hurricane, Spectra-Physics) was focused under an inverted microscope (IX71, Olympus, Tokyo, Japan) with a ×20 objective lens (Olympus, N.A. 0.46) on the MPC polymer-layered substrate immersed in water, phosphate-buffered saline (pH 7.4), or culture medium. The scanning rate of the femtosecond laser beam was 20 μm s^{-1}. The MPC polymer-layered substrate was scratched at 1 or 2 μm intervals to form cytophilic domains.

Surface treatment with Q-dots

Surface modification of the MPC polymer-layered substrate was performed in water. After the layered substrate was blow-dried by N_2 gas, Q-dot solutions (100 nM in twice diluted PBS) were placed on the layered substrates and incubated for 16 h at 25 °C in a moisture chamber.

Surface treatment with fluorescent ECM proteins

The Alexa Fluor 488 collagen (0.2 μM, PBS) was placed on a layered substrate. Lines and diagrams were drawn on the layered substrate by the focused femtosecond laser beam. The patterned substrate was incubated in Alexa Fluor 488 collagen solution at 20–23 °C for 16 h and then washed with PBS. For multiple ECM treatment, the femtosecond laser was focused again on the substrate in PBS. The substrate was incubated under the same conditions in Alexa Fluor 555 laminin (0.1 μM). Fluorescence images were taken with a laser scanning microscope (Fluoview FV300; Olympus) at each step. The excitation wavelength was 488 nm. The fluorescence band was at 510–540 nm for Alexa Fluor 488 and at 570–695 nm for Alexa Fluor 555.

Culture of NHA on a patterned substrate

NHA that were pre-cultured on a culture flask surface were recovered by trypsinization and re-suspended in Lonza NHA medium. The patterned cytophilic domains were covered with collagen (0.1 μM in NHA medium). The NHA were seeded on the patterned cytophilic substrate with 1.5 × 10^4 cells cm^{-2}. After the cells adhered to the cytophilic domains on the laser patterned domains, the femtosecond laser was focused again on the MPC layer in medium containing collagen (0.1 μM). Culturing continued for 44 h after patterning new domains under conditions of 5% CO_2 and 95% humidity at 37 °C.

Co-culture of HeLa cells close to NHK on a patterned substrate

The NHK (1.5 × 10^4 cells cm^{-2}) were spread on an MPC polymer-layered substrate with several cytophilic domains (50 × 50 μm) and cultured for 16 h at 37 °C under 90% humidity and 5% CO_2 in a medium (EpLife-KG2 medium diluted with the same volume of DMEM containing 5% FBS, gelatin (1 mg ml^{-1}), insulin (5 μg ml^{-1}), human epidermal growth factor (hEGF) (50 pg ml^{-1}), hydrocortisone (250 ng ml^{-1}), gentamycin (25 μg ml^{-1}), amphotericin B (25 ng ml^{-1}), bovine pituitary extract (0.2% v/v), and FBS (5%)). New cytophilic domains (50 × 50 μm) were formed close to the NHK by femtosecond laser ablation. The HeLa cells were individually transported to the newly prepared cytophilic domains by femtosecond laser-induced impulsive force, a non-contact cell handling method.[35,36] The NHK and HeLa cells were co-cultured in the same medium. The cell behavior was monitored at 30 min intervals.

SEM analysis

The SEM images were collected with an SM 7400F (JEOL, Akishima, Japan) at 1.0 kV accelerated voltage.

XPS analysis

Surface elements of the ablated and non-ablated substrates were identified with an AXIS Spectrometer (Kratos, Manchester, UK) using Al radiation (1486.6 eV, pass energy: 40 eV). Signals were resolved by a Gaussian–Lorenzian peak model, and corrected for binding energy of C 1s (284.8 eV for hydrogen groups).[42] Surface compositions were estimated using the XPS Database of the National Institute of Standards and Technology (NIST).[42]

Acknowledgements

This work was supported by a Grant-in-Aid for Scientific Research (B) (No. 20310075) to KO from the Japan Society for the Promotion of Science, by a program funding basic research centers in a private university from the Ministry of Education, Culture, Sports, Science and Technology (MEXT) of Japan to the Kansei Fukushi Research Institute, Tohoku Fukushi University (2008–2012), and by a grant to HT from the Research Foundation for Opto-Science and Technology. KO, YKL, and HM thank the National Science Council of the Republic of China, Taiwan, for its financial support and the Ministry of Education Taiwan under the Aim for Top University project (the MOE ATU project) to NCTU. FJK also

thanks the MOE ATU project (NYMU). The MPC polymer was kindly gifted by NOF Corporation (Tokyo, Japan). The authors thank Mr. Yasuo Okajima and Mr. Noritaka Koike of NAIST for XPS and SEM analysis, respectively. Ted Knoy is appreciated for his editorial assistance.

References

1 M. Schena, D. Shalon, R. W. Davis and P. O. Brown, *Science*, 1995, **270**, 467–470.
2 S. P. A. Fodor, R. P. Rava, X. C. Huang, A. C. Pease, C. P. Holmes and C. L. Adams, *Nature*, 1993, **364**, 555–556.
3 B. T. Houseman, J. H. Huh, S. J. Kron and M. Mrksich, *Nat. Biotechnol.*, 2002, **20**, 270–274.
4 G. MacBeath and S. L. Schreiber, *Science*, 2000, **289**, 1760–1763.
5 P. Uetz, L. Giot, G. Cagney, T. A. Mansfield, R. S. Judson, J. R. Knight, D. Lockshon, V. Narayan, M. Srinivasan, P. Pochart, A. Qureshi-Emili, Y. Li, B. Godwin, D. Conover, T. Kalbfleisch, G. Vijayadamodar, M. Yang, M. Johnston, S. Fields and J. M. Rothberg, *Nature*, 2000, **403**, 623–627.
6 H. Moriguchi, Y. Wakamoto, Y. Sugio, K. Takahashi, I. Inoue and K. Yasuda, *Lab Chip*, 2002, **2**, 125–130.
7 D. Kleinfeld, K. H. Kahler and P. E. Hockberger, *J. Neurosci.*, 1988, **8**, 4098–4120.
8 Y. Tsuda, T. Shimizu, M. Yamato, A. Kikuchi, T. Sasagawa, S. Sekiya, J. Kobayashi, G. Chen and T. Okano, *Biomaterials*, 2007, **28**, 4939–4946.
9 W.-S. Yeo, C. D. Hodneland and M. Mrksich, *ChemBioChem*, 2001, **2**, 590–593.
10 J. Nakanishi, T. Takarada, K. Yamaguchi and M. Maeda, *Anal. Sci.*, 2008, **24**, 67–72.
11 J. Robertus, W. R. Browne and B. L. Feringa, *Chem. Soc. Rev.*, 2010, **39**, 354–378.
12 H. Kaji, K. Tsukidate, M. Hashimoto, T. Matsue and M. Nishizawa, *Langmuir*, 2005, **21**, 6966–6969.
13 S. S. Shah, J. Y. Lee, S. Verkhoturov, N. Tuleuova, E. A. Schweikert, E. Ramanculov and A. Revzin, *Langmuir*, 2008, **24**, 6837–6844.
14 Y. Kikuchi, J. Nakanishi, T. Shimizu, H. Nakayama, S. Inoue, K. Yamaguchi, H. Iwai, Y. Yoshida, Y. Horiike, T. Takarada and M. Maeda, *Langmuir*, 2008, **24**, 13084–13095.
15 S. Petersen, J. M. Alonso, A. Specht, P. Duodu, M. Goeldner and A. del Campo, *Angew. Chem. Int. Ed.*, 2008, **47**, 3192–3195.
16 S. Yamaguchi, S. Yamahira, K. Kikuchi, K. Sumaru, T. Kanamori and T. Nagamune, *Angew. Chem. Int. Ed.*, 2012, **51**, 128–131.
17 G. Pasparakis, T. Manouras, A. Selimis, M. Vamvakaki and P. Argitis, *Angew. Chem. Int. Ed.*, 2011, **50**, 4142–4145.
18 S. J. Todd, D. J. Scurr, J. E. Gough, M. R. Alexander and R. V. Ulijn, *Langmuir*, 2009, **25**, 7533–7539.
19 D. Liu, Y. Xie, H. Shao and X. Jiang, *Angew. Chem. Int. Ed.*, 2009, **48**, 4406–4408.
20 J. Edahiro, K. Sumaru, Y. Tada, K. Ohi, T. Takagi, M. Kameda, T. Shinbo, T. Kanamori and Y. Yoshimi, *Biomacromolecules*, 2005, **6**, 970–974.
21 W. Luo and M. N. Yousaf, *J. Am. Chem. Soc.*, 2011, **133**, 10780–10783.
22 A. Vogel, J. Noack, G. Hüttman and G. Paltauf, *Appl. Phys. B*, 2005, **81**, 1015–1047.
23 Y. Hosokawa, M. Yashiro, T. Asahi and H. Masuhara, *J. Photochem. Photobiol. A: Chemistry*, 2001, **142**, 197–207.
24 H. Jeon, R. Schmidt, J. E. Barton, D. J. Hwang, L. J. Gamble, D. G. Castner, C. P. Grigoropoulos and K. E. Healy, *J. Am. Chem. Soc.*, 2011, **133**, 6138–6141.
25 N. Hartmann, S. Franzka, J. Koch, A. Ostendorf and B. N. Chichkov, *Appl. Phys. Lett.*, 2008, **92**, 223111.
26 V. Dinca, M. Farsari, D. Kafetzopoulos, A. Popescu, M. Dinescu and C. Fotakis, *Thin Solid Films*, 2008, **516**, 6504–6511.
27 S. Catros, J.-C. Fricain, B. Guillotin, B. Pippenger, R. Bareille, M. Remy, E. Lebraud, B. Desbat, J. Amédée and F. Guillemot, *Biofabrication*, 2011, **3**, 025001.
28 B. R. Ringeisen, H. Kim, J. A. Barron, D. B. Krizman, D. B. Chrisey, S. Jackman, R. Y. C. Auyeung and B. J. Spargo, *Tissue Eng.*, 2004, **10**, 483–491.
29 Y. Hosokawa, T. Kaji, C. Shukunami, Y. Hiraki, E. Kotani, H. Mori and H. Masuhara, *Biomed. Microdevices*, 2007, **9**, 105–111.
30 T. Kaji, S. Ito, H. Miyasaka, Y. Hosokawa, H. Masuhara, C. Shukunami and Y. Hiraki, *Appl. Phys. Lett.*, 2007, **91**, 023904.
31 Y. Liu, S. Sun, S. Singha, M. R. Cho and R. J. Gordon, *Biomaterials*, 2005, **26**, 4597–4605.
32 G. D. Pins, K. A. Bush, L. P. Cunningham and P. J. Campagnola, *J. Biomed. Mater. Res. Part A*, 2006, **78A**, 194–204.
33 B. Kaehr and J. B. Shear, *Proc. Natl. Acad. Sci. USA*, 2008, **105**, 8850–8854.
34 H. Yasuda, N. Shima, N. Nakagawa, K. Yamaguchi, M. Kinosaki, S. Mochizuki, A. Tomoyasu, K. Yano, M. Goto, A. Murakami, E. Tsuda, T. Morinaga, K. Higashio, N. Udagawa, N. Takahashi and T. Suda, *Proc. Natl. Acad. Sci. USA*, 1998, **95**, 3597–3602.
35 K. Okano, D. Yu, A. Matsui, Y. Maezawa, Y. Hosokawa, A. Kira, M. Matsubara, I. Liau, H. Tsubokawa and H. Masuhara, *ChemBioChem*, 2011, **12**, 795–801.
36 H. Yamamoto, K. Okano, T. Demura, Y. Hosokawa, H. Masuhara, T. Tanii and S. Nakamura, *Appl. Phys. Lett.*, 2011, **99**, 163701.
37 J. Sibarani, M. Takai and K. Ishihara, *Colloid Surf. B-Biointerfaces*, 2007, **54**, 88–93.
38 T. Uchida, N. Shimo, H. Sugimura and H. Masuhara, *J. Appl. Phys.*, 1994, **76**, 4872–4878.
39 S. H. Behrens and D. G. Grier, *J. Chem. Phys.*, 2001, **115**, 6716–6721.
40 A. Kumar, A. B. Mandale and M. Sastry, *Langmuir*, 2000, **16**, 6921–6926.
41 N. Kaneko, O. Marín, M. Koike, Y. Hirota, Y. Uchiyama, J. Y. Wu, Q. Lu, M. Tessier-Lavigne, A. Alvarez-Buylla, H. Okano, J. L. R. Rubenstein and K. Sawamoto, *Neuron*, 2010, **67**, 213–223.
42 *NIST X-ray Photoelectron Spectroscopy Database: NIST Standard Reference Database 20, Version 3.5*, the National Institute of Standards and Technology (NIST), http://srdata.nist.gov/xps/.

